Hindawi
Journal of Function Spaces
Volume 2023, Article ID 9876837, 1 page
https://doi.org/10.1155/2023/9876837

Retraction

Retracted: The Experimental Validation of a Digital Filter Mathematical Modelling for Nuclear Fuel Vibration Monitoring System

Journal of Function Spaces

Received 15 August 2023; Accepted 15 August 2023; Published 16 August 2023

This article has been retracted by Hindawi following an investigation undertaken by the publisher [1]. This investigation has uncovered evidence of one or more of the following indicators of systematic manipulation of the publication process:

(1) Discrepancies in scope

(2) Discrepancies in the description of the research reported

(3) Discrepancies between the availability of data and the research described

(4) Inappropriate citations

(5) Incoherent, meaningless and/or irrelevant content included in the article

(6) Peer-review manipulation

The presence of these indicators undermines our confidence in the integrity of the article's content and we cannot, therefore, vouch for its reliability. Please note that this notice is intended solely to alert readers that the content of this article is unreliable. We have not investigated whether authors were aware of or involved in the systematic manipulation of the publication process.

Wiley and Hindawi regrets that the usual quality checks did not identify these issues before publication and have since put additional measures in place to safeguard research integrity.

We wish to credit our own Research Integrity and Research Publishing teams and anonymous and named external researchers and research integrity experts for contributing to this investigation.

The corresponding author, as the representative of all authors, has been given the opportunity to register their agreement or disagreement to this retraction. We have kept a record of any response received.

References

[1] H. Yong, H. Shiyong, H. MengXuan et al., "The Experimental Validation of a Digital Filter Mathematical Modelling for Nuclear Fuel Vibration Monitoring System," *Journal of Function Spaces*, vol. 2022, Article ID 9741419, 11 pages, 2022.

Hindawi
Journal of Function Spaces
Volume 2022, Article ID 9741419, 11 pages
https://doi.org/10.1155/2022/9741419

Research Article

The Experimental Validation of a Digital Filter Mathematical Modelling for Nuclear Fuel Vibration Monitoring System

Han Yong,[1] **Huang Shiyong**,[2] **Han MengXuan**,[3] **Zhao Tao**,[1] **Wen Guang**,[1] **Gu Mingfei**,[4] **and Zhang Qi**[1,5]

[1]*Chengdu Vocational & Technical College of Industry, Chengdu 610218, China*
[2]*Chengdu China Nuclear Haichuan Nuclear Technology Co., Ltd., Chengdu 610041, China*
[3]*University of Electronic Science and Technology of China, Chengdu 610041, China*
[4]*Science and Technology on Reactor System Design Technology Laboratory, Nuclear Power Institute of China, Chengdu 610213, China*
[5]*School of Intelligent Manufacturing, Panzhihua College, Panzhihua 617000, China*

Correspondence should be addressed to Zhang Qi; pzhuzq@stu.scu.edu.cn

Received 4 April 2022; Revised 10 May 2022; Accepted 16 May 2022; Published 4 June 2022

Academic Editor: Miaochao Chen

Aiming at vehicles will produce shocks and vibrations for various reasons in the process of transportation and handling, any shock and vibration that exceeds the regulations would cause damage to the nuclear fuel being transported. In order to monitor and analyze the shock and vibration data scientifically, a monitoring system based on MEMS acceleration sensor technology is developed to measure shocks and vibrations. The measured result involves some noise caused by the sensitivity of the sensor and the electrical noise, and a digital filter mathematical modelling is introduced to reduce noise and improve the measured result accuracy. In order to verify the effectiveness of the device designed in this paper, the device and the high-precision seismic acceleration sensor AC73 are, respectively, used for field tests; the results show that the test precision of the designed device can meet the requirements, and also, the designed shock and vibration monitoring system can record and store the three-axis acceleration, temperature, humidity, pressure, time, and other parameters that exceed the set threshold during nuclear fuel transportation in real time and complete the fuel assembly transportation status assessment and promptly remind the transportation personnel to take safety precautions and treatment measures. Therefore, it can be widely used in the monitoring, recording, and postevent data analysis of the transportation process of important products such as nuclear fuel.

1. Introduction

Nuclear fuel is expensive and easy to be impacted and vibrated during transportation, which will affect its use. Therefore, the internal or external damage monitoring of nuclear fuel caused by various shocks and vibrations during nuclear fuel transportation should be fully considered. In order to ensure the safety of nuclear fuel transportation, special vehicles and professional drivers are generally used for speed limited transportation, supplemented by mechanical accelerometers as the indication of exceeding the acceleration limit. The mechanical accelerometer, as the auxiliary monitoring of shocks and vibrations, can indicate whether the acceleration exceeds the limit, but it cannot give information about the specific value and occurrence time of the acceleration suffered by the fuel assembly and will not give an early warning. Due to the complex transportation conditions, professional drivers need to often check the road conditions before deciding on subsequent operations; mechanical accelerometers cannot provide monitoring data records as postanalysis, which is lack of scientificity. Therefore, it is necessary to use advanced sensor technology and monitoring technology to design a safe, efficient, and scientific nuclear fuel transportation monitoring system. Senodia Technologies has independent intellectual property rights of commercial MEMS inertial sensor production technology, and MEMSIC Inc. (USA) developed products that integrate MEMS and signal processing circuits into a single chip. Liu

Huijuan of Ocean University of China and others carried out the design of vibration monitoring system based on MEMS [1]. Zhang Jiangang of China Academy of Radiation Protection and others carried out the experience summary of test verification of radioactive goods transport containers [2, 3]. Xu Lei of the Army Engineering University and others carried out research on the design of vibration acceleration measurement system based on MEMS acceleration sensor [4]. By far, the acceleration monitoring technology of ordinary commercial transportation has gradually integrated into the domestic general logistics transportation, mechanical and electronic manufacturing, automobile manufacturing, and other fields and has achieved certain application results. However, there are relatively fewer reports on the acceleration monitoring of fuel assembly transportation in nuclear power plant.

According to the requirements of fuel assembly transportation acceleration and fuel assembly special transportation container and the special requirements of fuel assembly transportation container, a low-power digital fuel assembly transportation container acceleration monitoring system (hereinafter referred to as transportation acceleration monitoring system) based on MEMS acceleration sensor and single-chip microcomputer technology is designed, as it has the function of real-time automatic recording and storage of acceleration information in the whole transportation process, and it can timely help the transportation personnel take safety precautions and facilitate subsequent analysis and summary and meet the requirements of nuclear fuel safety transportation analysis [5–9].

2. System Design

2.1. Technical Requirement of Shock and Vibration Acceleration Recorder

(1) Acceleration (triaxial): range: 0~±10 g/±20 g/±40 g, settable; nonlinearity: ±0.1% FSR (±10 g) and ±1.3% FSR (±40 g)

(2) It has RS232 serial computer interface and alarm indication output interface

(3) The power is not more than 90 MW, the battery power supply mode, and the continuous working time is more than 15 days

(4) Overall weight: no more than 1.5 kg; size: no more than 110 ∗ 100 ∗ 80 mm

2.2. System Working Process

(1) Before the transportation of nuclear fuel and other valuables, take out the shock and vibration acceleration recorder, activate it through PC monitoring application software, and install and fix it on the transported equipment for transportation process monitoring

(2) In the process of transportation, in case of shocks and vibrations, the shock and vibration acceleration recorder measures its value through the integrated temperature, humidity, pressure, and triaxial acceleration sensors, triggers recording and alarm when it exceeds the set value, reminds the transportation personnel to pay attention, and stores the temperature, humidity, pressure, triaxial acceleration, and corresponding time when it exceeds the threshold

(3) After transportation, remove the shock and vibration acceleration recorder from the transported equipment, and then, use PC monitoring application software to read the recorded data for relevant analysis, so as to mine the value of the data, improve the transportation quality, and reduce losses

Its schematic diagram of system working process is shown in Figure 1.

2.3. The Shock and Vibration Acceleration Recorder Design

2.3.1. Selection and Calculation of Key Technologies

(1) MEMS Triaxial Acceleration Sensor. The MEMS triaxial acceleration sensor selects the programmable maximum shock and vibration measurement range of ±20 g and ±40 g.

(2) Battery Capacity. In the actual process of nuclear fuel transportation, fuel assemblies are often transported through the combination of special railway line and road transportation. According to the layout of China's nuclear fuel supply and use enterprises, the single transportation distance of nuclear fuel is up to 2000 or 3000 kilometers, and the transportation time lasts about 7 days. The working time of 15 days needs to be considered. The calculation formula of battery capacity is as follows:

$$Q = \frac{P \times t}{k \times U}, \tag{1}$$

where Q is the required lithium battery capacity (Ah), P is the load power (W), t is the daily electricity hours, U is the standard lithium battery voltage, and k is the discharge control coefficient (0.75~0.8).

The main chip power consumption is shown in Table 1.

According to Table 1, the total power consumption is 22.91 mA, calculated as 25 mA, and the voltage is calculated according to the working voltage of 3.7 V; then,

$$Q1 = \frac{25 * 24 * 15}{0.75 * 3.7} = 3244\ \text{mAh}. \tag{2}$$

Considering that the circuit needs voltage transformation, and the comprehensive efficiency is taken as 50%, the following can be obtained:

$$Q = \frac{Q1}{0.5} = 6488\ \text{mAh}. \tag{3}$$

Therefore, two 18650 type rechargeable lithium batteries with a nominal voltage of 3.7 V and capacity of 3400 mAh

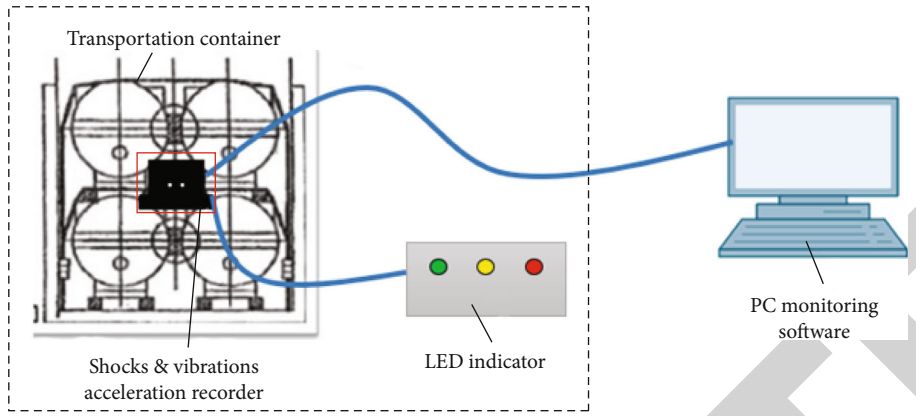

Figure 1: Schematic diagram of system working process.

Table 1: Main chip power consumption.

Name	Power consumption (mA)	Remark
MCU (ARM)	12.8	16 MHz operation
Triaxial acceleration sensor	0.15	
Storage	0.7	It is estimated that 10% of the time will be spent reading and writing data
Pressure sensor	4	
Temperature and humidity sensor	0.5	
LDO power supply and power reference	0.46	
Serial port protection chip	1	
Optical coupling relay	3.3	The outputs are mutually exclusive, with only one output at a time

can ensure the normal operation of the shock and vibration acceleration recorder for 15 days.

2.3.2. Mechanical Structure Design. In order to ensure the strength and measurement accuracy of the product, the shock and vibration acceleration recorder is designed with a compact structure, which is composed of an upper cover plate and an integrated base. The integrated base is divided into three parts according to the structure and function; from bottom to top are circuit board installation area, baffle plate, and battery area. The sensor measuring board and main board are fixed in the circuit board installation area, the upper side of the main board is equipped with a baffle plate which plays the role of support and electromagnetic interference shielding, two large capacity rechargeable lithium batteries are placed on the baffle plate, and an upper cover plate is placed on the upper part of the battery. The upper cover plate and the integrated base are compacted with 4 fastening screws through the sealant strip to ensure the reliable fixation of the battery and provide the IP65 protection function of the instrument. The integrated base is provided with a connecting hole, which can be fixed to the transportation parts with screws during operation. The overall dimension of the shock and vibration acceleration recorder is about 105 mm (length) × 86 mm (width) × 65 mm (high). The effect diagram is shown in Figure 2.

2.3.3. Electronic Circuit Design. The electronic circuit is the core part of the shock and vibration acceleration recorder, which undertakes the role for measurement, recording, and storage of triaxial shock and vibration acceleration, temperature, humidity, and atmospheric pressure. Its principle block diagram is shown in Figure 3.

In order to ensure the accuracy of triaxial shock and vibration measurement and reduce mutual interference, the measurement motherboard and sensor board are arranged separately. The measurement motherboard completes the measurement of temperature, humidity, atmospheric pressure, battery power, and other parameters, and the measurement motherboard is connected with the outside through the alarm interface and data interface. The sensor board adopts the three-axis integrated design to complete the three-axis shock and vibration measurement. The measurement motherboard and the sensor board are connected through a special interface with a flexible line. The PCB effect diagram of the shock and vibration acceleration recorder is shown in Figure 4.

2.3.4. Program Design

(1) Program Function Design. The shock and vibration acceleration recorder reads the data of the triaxial acceleration sensor in real time. Compared with the set alarm threshold,

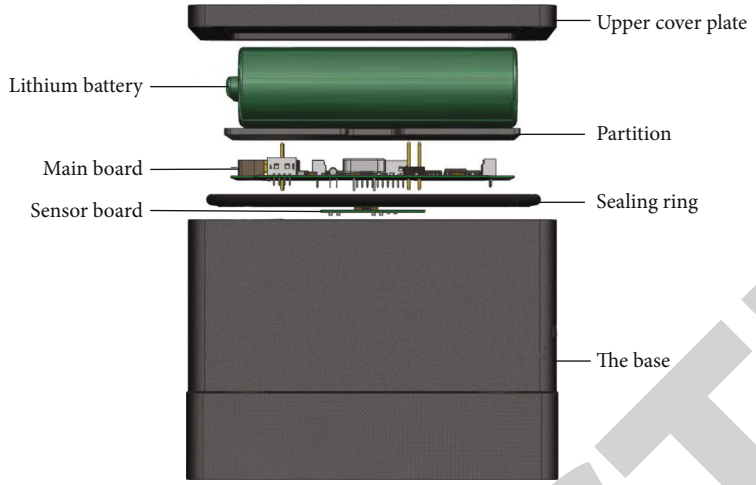

Figure 2: Mechanical appearance effect diagram.

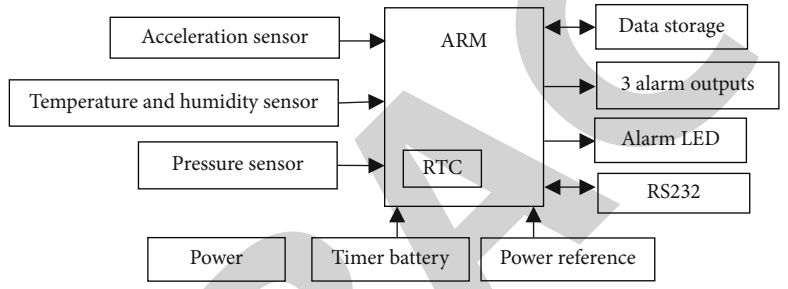

Figure 3: The principle block diagram of the shock and vibration acceleration recorder.

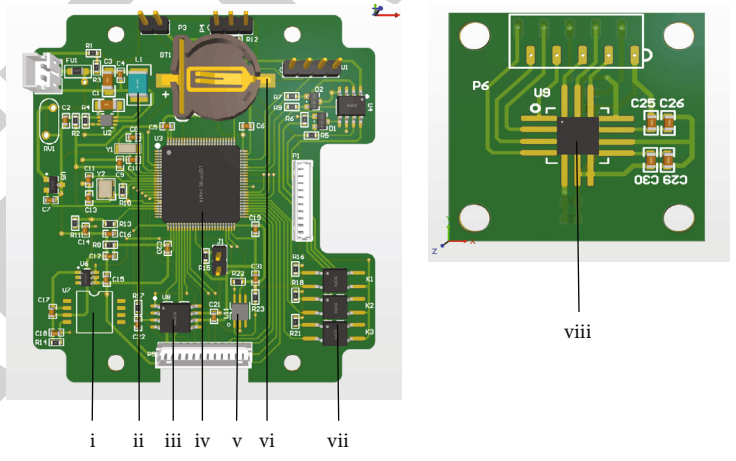

Figure 4: The PCB effect diagram of the shock and vibration acceleration recorder. (a) Motherboard with (A) pressure measurement, (B) LDO power, (C) storage, (D) ARM, (E) humidity and temperature measurement, (F) timer battery, and (G) alarm output. (b) Sensor board with (A) acceleration MEMS sensor.

it is greater than the set alarm threshold and drives the alarm circuit to work. At the same time, relevant parameters (current time, triaxial acceleration, temperature, humidity, and pressure) are stored and respond to computer commands and other operations at an appropriate time. The software block diagram is shown in Figure 5.

(2) Filtering method and algorithm.

(a) The built-in low-pass antialiasing filter of the three-axis acceleration sensor realizes the hardware filtering of the analogue signal to ensure that the output signal eliminates the noise and interference caused

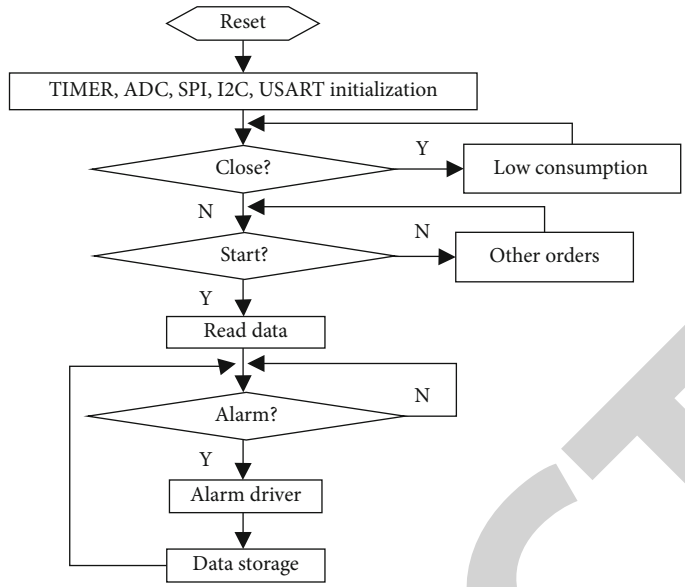

Figure 5: Program block diagram of the shock and vibration acceleration recorder.

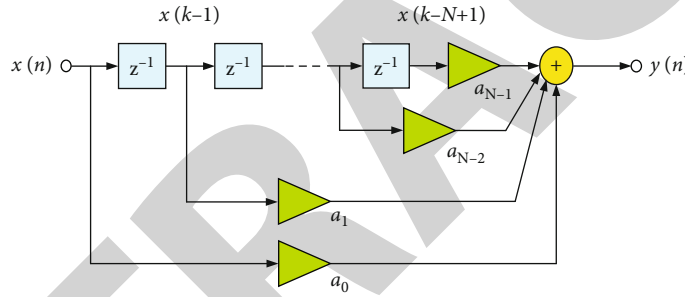

Figure 6: Implementation principle of FIR.

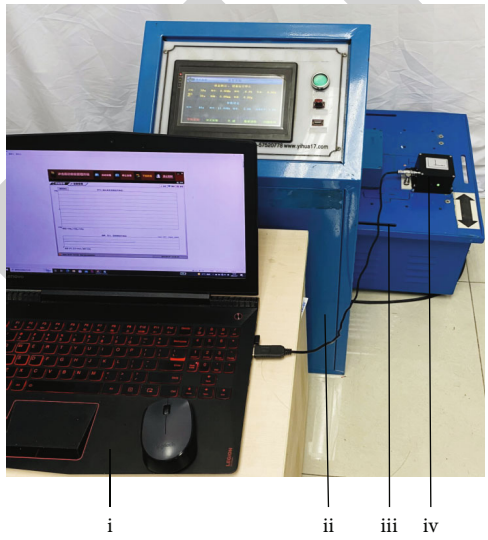

Figure 7: Function and performance test picture. (a) PC monitoring. (b) Vibration test console. (c) Vibration test platform. (d) Shock and vibration acceleration recorder.

by the sensor itself. After A/D conversion, ARM is used to program the low-pass and high-pass filters of MEMS sensor to realize hardware digital filtering to ensure that the output signal is clean and is a digital signal within the required frequency range

(b) FIR filtering algorithm further removes unwanted interference signals. The algorithm to realize the filter is usually realized by FIR or IIR. The main feature of FIR filter is that there is no feedback loop and no instability problem. While the amplitude characteristic is set arbitrarily, the accurate linear phase can be guaranteed, and the software and hardware are easy to realize. The filter transition process has a finite interval. Compared with IIR filter, the disadvantage is higher order and larger delay than IIR filter with the same performance. The advantage of IIR filter is that it can achieve better filtering effect at the same order, but the disadvantage of IIR filter design method is that it cannot control the phase characteristics of the filter and the filter may be unstable. Therefore, FIR filter is generally used as adaptive filter. FIR filter is a LTI (linear time invariant) digital

Table 2: Repeatability test data of acceleration recorder (z-axis, unit: g).

Value (g)									
0.84	-0.92	0.82	-0.88	0.85	-0.89	0.84	-0.89	0.8	-0.87
0.81	-0.9	0.88	-0.92	0.81	-0.89	0.81	-0.92	0.85	-0.95
0.82	-0.9	0.81	-0.91	0.85	-0.95	0.84	-0.92	0.8	-0.88
0.84	-0.92	0.82	-0.9	0.81	-0.89	0.82	-0.9	0.85	-0.91
0.85	-0.89	0.85	-0.92	0.85	-0.9	0.81	-0.91	0.82	-0.91
0.85	-0.92	0.81	-0.89	0.84	-0.91	0.8	-0.89	0.82	-0.9
0.82	-0.91	0.82	-0.89	0.82	-0.91	0.82	-0.91	0.82	-0.89
0.82	-0.91	0.82	-0.9	0.81	-0.91	0.85	-0.92	0.82	-0.91
0.85	-0.89	0.81	-0.91	0.82	-0.91	0.85	-0.9	0.85	-0.9

filter with constant coefficients. Its implementation principle is shown in Figure 6.

The relationship between FIR output with length N and input time series $X(n)$ is given in the form of finite convolution sum. The specific form is as follows:

$$y(n) = \sum_{n=0}^{N-1} (a(n) \times x(k-n)),$$
$$a(n) = \frac{6}{N(N+1)} \times \left(1 - \frac{2n}{N-1}\right) n = 0, 1, \cdots, N-1. \quad (4)$$

The shock and vibration acceleration recorder uses ARM as the control core and is a mobile product, which needs to balance performance and power consumption. Therefore, it is very reasonable to select FIR within the tenth order for filtering to better remove the interference signal

(c) The piecewise linear coefficient compensation algorithm is used to calibrate the collected and processed signal to ensure that the linearity and error of the output signal in the whole measurement range are within the allowable range of the national standard. After the filtering of the above software and hardware, the signal of the impact vibration acceleration recorder has been relatively clean. In order to ensure the linearity and accuracy of the signal, we designed the linear coefficient compensation method to calibrate it. Use $y = ax + b$ to correct the acceleration values of three axes, respectively, namely,

$$\begin{pmatrix} x \\ y \\ z \end{pmatrix} = \begin{pmatrix} a \\ b \\ c \end{pmatrix} \times \begin{pmatrix} x \\ y \\ z \end{pmatrix} + \begin{pmatrix} d1 \\ d2 \\ d3 \end{pmatrix}. \quad (5)$$

The specific method is as follows: use the data management software to write the coefficients a, b, c, $d1$, $d2$, and $d3$ into the impact vibration acceleration recorder. The recorder uses the above formula to correct and remove the DC offset to further ensure the linearity and accuracy of acceleration measurement

(d) The least square method is used to fit the temperature compensation algorithm. The shock and vibration acceleration recorder uses the temperature sensor to detect the working environment temperature of the product. ARM uses the measured working environment temperature and uses the least square method to fit the temperature compensation algorithm according to the temperature curve of the acceleration sensor for correction, which can ensure that the product has good linearity and accuracy in different working temperature environments

(3) Communication Protocol. The computer as the host adopts USB interface. As a slave, the shock and vibration acceleration recorder adopts TTL level duplex serial port communication mode. Data communication format: 115200, N, 8,1. Verification method: use cumulative sum to take the lower byte. Cumulative sum data: function code +data length+data. The command format is as follows: start bit (0xFDFD), function code 1 byte, data length 2 bytes, data n byte, and check 1 byte.

3. Experiment Verification and Data Analysis

3.1. Experiment Methods. Fix the shock and vibration acceleration recorder and Ultrashock/AC-73 product on the vibration test platform and connect it to PC with communication cable; open and execute the PC monitoring application software, and start the test. The composition of the test system is shown in Figure 7.

3.2. Repeatability Test of Acceleration Measurement. The vibration test platform outputs a stable acceleration excitation source, and a total of 90 data are collected at the same point (as shown in Table 2). The range of positive acceleration in z-axis is 0.8~0.85, the mean value is 0.828, and the maximum error of the mean value is 0.028. The range of negative acceleration in z-axis is -0.87~-0.91, the mean value is -0.905, and the maximum error of the mean value is 0.035. It can be seen that the resolution of the device is 0.01 and the repetition accuracy is less than 0.05 g.

3.3. Verification and Calibration Test of National Metering Station. The shock and vibration acceleration recorder was sent to China's national metrology station for verification and calibration. Its three-axis of XYZ was tested, 2G, 4G, and 6G were tested, respectively, and each parameter was tested for 10 times. The detection parameters should meet the requirements of amplitude error less than ±5% specified in JJG 676-2019 verification regulation of vibration meter. The detection errors are within the allowable error range of 5%, meet the technical requirements, and pass the verification of national metrology station. According to JJG676-2019 standard test procedure, CEPREI fixes the shock and vibration acceleration recorder on the standard test platform and tests the three-axis of XYZ of the shock and vibration

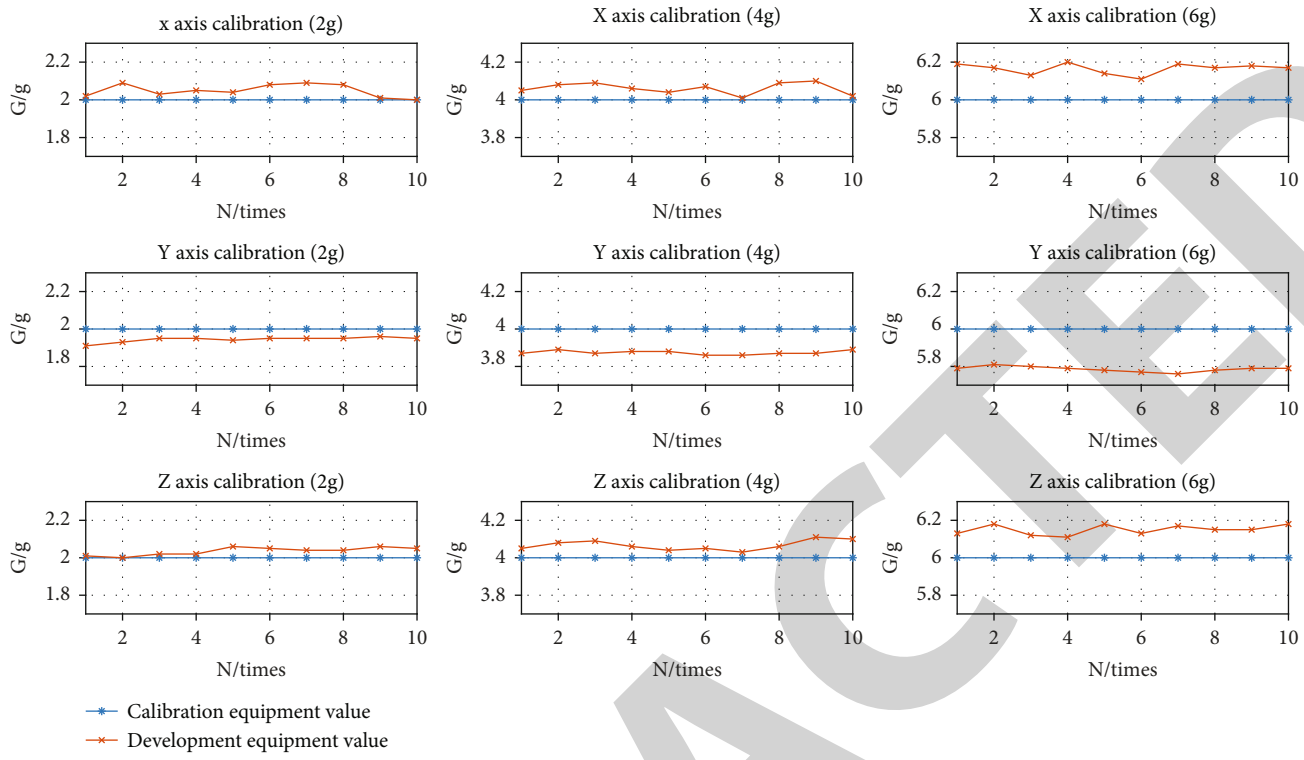

Figure 8: Axis calibration.

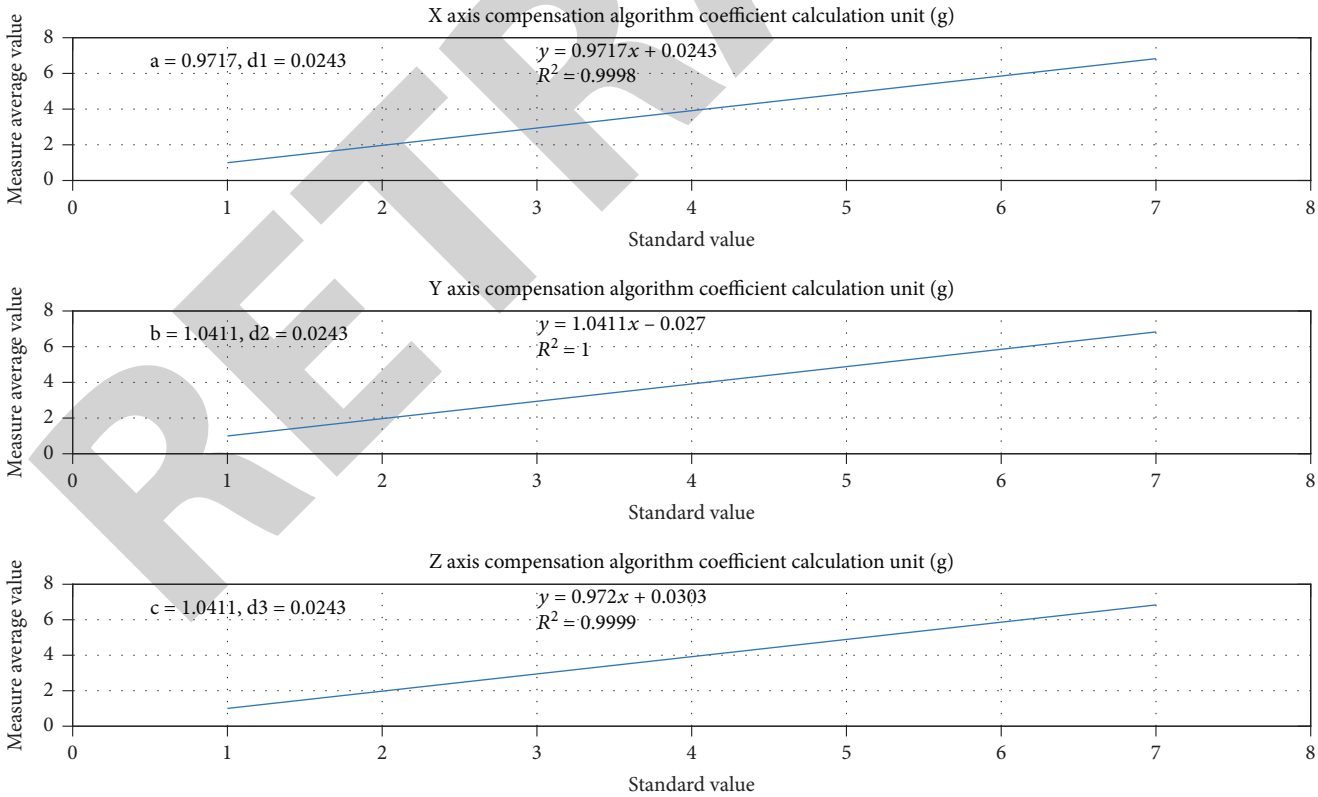

Figure 9: Compensation algorithm coefficient calculation of the shock and vibration acceleration recorder (top: x-axis calibration equation, middle: y-axis calibration equation, and bottom: z-axis calibration equation).

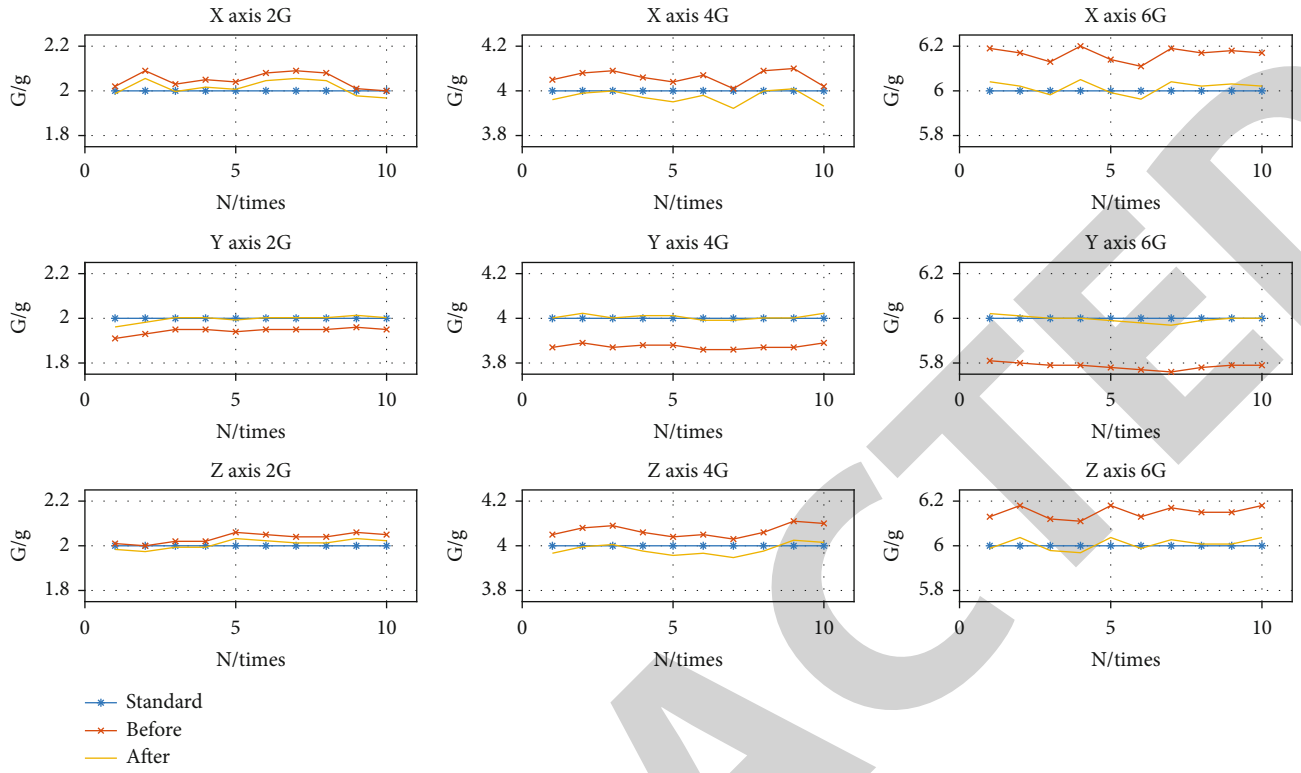

Figure 10: Comparison of measured and standard values of triaxial acceleration before and after linear coefficient compensation (blue: standard, red: before, and orange: after).

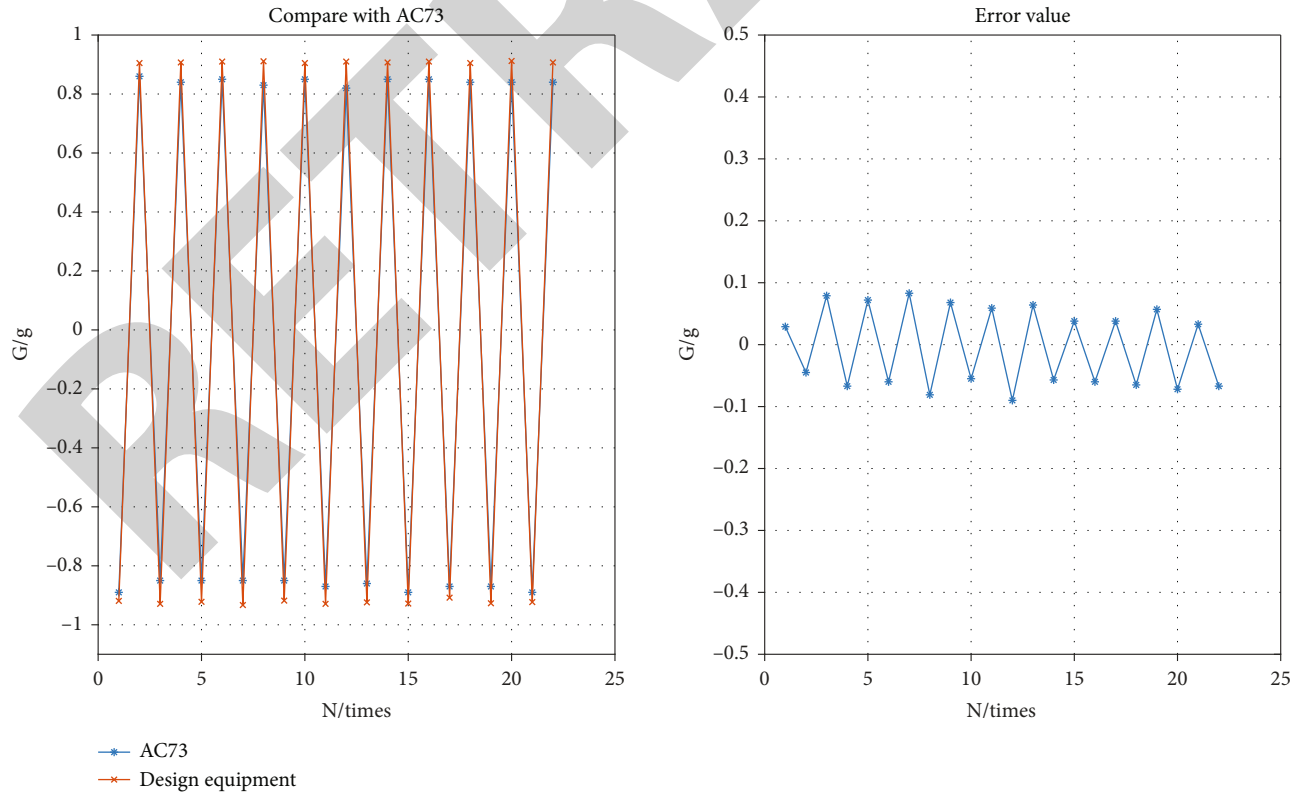

Figure 11: Measurement comparison test of the shock and vibration acceleration recorder and AC73 seismic acceleration sensor (vibration platform test data).

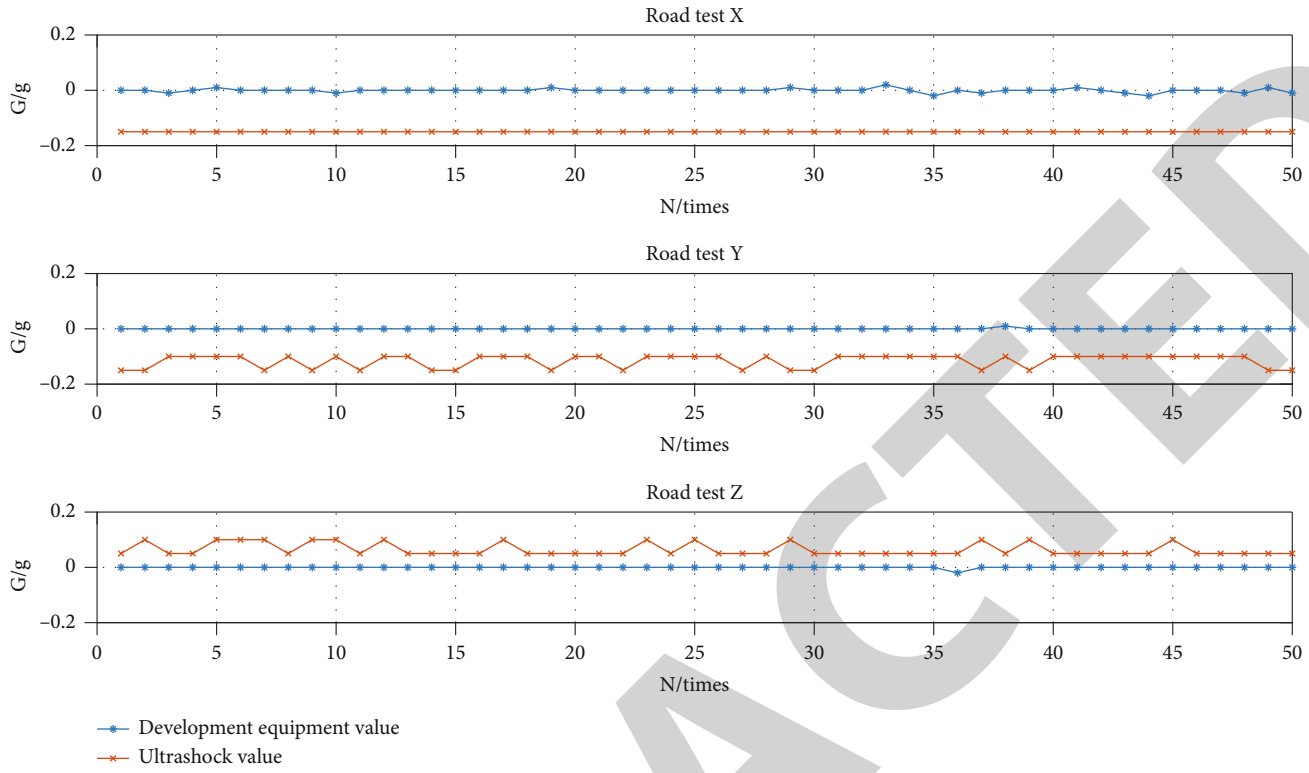

Figure 12: Road test comparison between the shock and vibration acceleration recorder and the similar foreign product acceleration measurement (first stage: beginning; second stage: work; and third stage: after transportation).

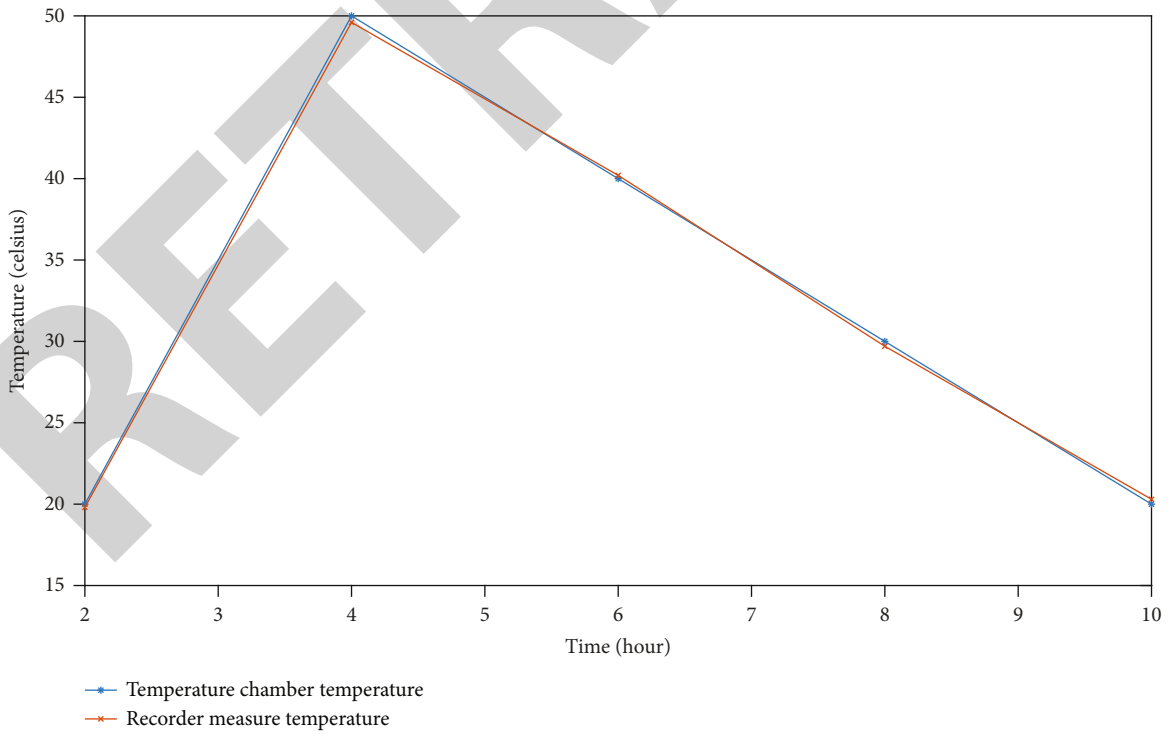

Figure 13: Temperature curve of environmental test.

acceleration recorder, 2G, 4G, and 6G were tested, respectively, and each parameter was tested for 10 times. The three-axis detection data is shown in Figure 8.

Taking the third-party calibration data as the standard, the linearity is calculated by Excel table, and the values of coefficient in Equation (5) are obtained, as shown in Figure 9.

Then, the linear coefficient is substituted into Excel table for simulation calculation. The results show that the accuracy of the shock and vibration acceleration recorder has been greatly improved. Except for individual discrete points, 95% numerical accuracy returns from 1%~5% to 0%~1%. Next, it is considered to implant the coefficient into the shock and vibration acceleration recorder through the computer monitoring software and send the product with the implanted coefficient to the third-party authority for recalibration to verify its effect. The comparison of measured acceleration before compensation, calculated acceleration after compensation, and standard value is shown in Figure 10.

3.4. Precision Test with High-Precision Seismic Acceleration Sensor AC73 as Reference. AC73 has higher performance than shock and vibration acceleration recorder and is very suitable for performance experiment verification as acceleration test benchmark. From the continuous vibration test in the z-axis direction, it can be seen that although the test is affected by the vibration platform, the z-axis test data of the two products have a certain deviation, the z-axis measurement values of the two products are relatively close, and the average error of the shock and vibration acceleration recorder relative to AC73 is 6%. The fluctuation error of the shock and vibration acceleration recorder is 4.7%. The fluctuation error of AC73 itself is 1.9%. Considering the different installation positions between the two and the influence of the vibration platform, after deducting the influence of the fluctuation error of AC73 itself, the average error between the two is less than 5% specified in JJG 676-2019, verification regulation of vibration meter. The sampling frequency of shock vibration acceleration recorder (512 Hz) and AC73 (1 kHz) is different, resulting in a certain time shift in the frequency reduction waveform. The actual time shift value is very small and can be ignored. After intercepting and graphing the maximum value, it can be seen that the two frequencies are consistent (see Figure 11).

3.5. Road Test with Ultrashock Logger. The shock and vibration acceleration recorder is placed on the vehicle together with similar foreign product for road test. Start the recorder before transportation and put them on the vehicle after getting on the vehicle (not rigidly fixed). After more than 1 hour of transportation (the transportation process time is 8:30~9:32), get off the vehicle, take out the two recorders, and read the data through their management software, as shown in Figure 12.

It can be seen from the comparison of measurement data of x-, y-, and z-axes:

(1) Function: both can start the recorder smoothly through the monitoring application software, correctly record and store data during the road test, and correctly read the data again through the monitoring application software after transportation

(2) Performance: before transportation, the data difference between the two is obvious because they are manually placed on the vehicle. During transportation, because the two recorders are not rigidly fixed on the vehicle (they are placed in different positions), the recorded data of the two recorders are different to some extent. Generally speaking, the data of x-axis and y-axis are close, and there are some differences in z-axis (in most cases, the absolute value of the shock and vibration acceleration recorder is slightly smaller than that of the similar foreign product at the same measuring point), but the recording trend of the two is basically the same (the high and low values are basically the same). After transportation, the two are removed from the vehicle due to manual placement, and the recorded data are obviously different

3.6. Environmental Test. The environment test step is described as follows: first, get the value from the shock and vibration acceleration recorder to make sure the recorder can work in normal. And keep the recorder work in the whole process. Second, put the recorder into the temperature test chamber, and manipulate the temperature test chamber to raise the temperature. Third, when the temperature reaches the highest point, make sure the recorder work in normal. Fourth, decrease the temperature. The environmental test temperature curve is in Figure 13.

After the test, it can be seen that the shock and vibration acceleration recorder can normally measure acceleration, temperature, humidity, and pressure in the whole process.

3.7. Electromagnetic Compatibility Test. According to GB/Z17799.6-2017, GB/T17626.2-2018, and GB/T17626.4-2008, the immunity bench is used for shell immunity test (considering 6 kV contact or 8 kV air discharge) and signal port immunity test (considering 1 kV port contact). It can be seen from the EMC test results that the design of shielding with metal shell plays a good role in electromagnetic shielding and has withstood the test in the immunity test of shell and signal port.

4. Conclusions

For the purpose of engineering reliability and stability, considering the economic practicability, the shock and vibration monitoring system of nuclear fuel transportation is designed by using MEMS sensor acceleration measurement method and system monitoring application software, which can better meet the requirements of nuclear fuel transportation process monitoring.

After the monitoring system is started, the shock and vibration acceleration recorder can automatically complete the functions of measurement, recording, out of limit

storage, and alarm in the transportation process of nuclear fuel. The monitoring application software can complete data transfer, query, print, and restore the transportation process records. The whole transportation process is monitored by the shock and vibration acceleration recorder, which reduces the labor intensity and human factor error of transportation workers and improves the work efficiency and transportation quality.

The modular design idea is fully integrated into the design of the system, and the sensor expansion interface is reserved, which can facilitate the subsequent addition of attitude detection. With the addition of various sensor measuring boards, the transportation process monitoring with different functions can be realized to meet the needs of customers in various industries.

Data Availability

The data used to support the findings of this study are available from the corresponding author upon request.

Conflicts of Interest

The authors declare that they have no known competing financial interests or personal relationships that could have appeared to influence the work reported in this paper.

Acknowledgments

The authors would like to thank Chen Fei for the test work. This work was sponsored by the Science and Technology Plan Project of Sichuan Province under contract (No. 2021YJ0058) and Artificial Intelligence Key Laboratory of Sichuan Province (No. 2021RYY01).

References

[1] H.-j. Liu and X. Li, "Design of vibration detecting system based on MEMS," *Modern Electronic Technology*, vol. 34, no. 22, pp. 77–79, 2011.

[2] J. Zhang, L. Guoqiang, H. Sun, D. Zhuang, S. Sun, and D. Meng, "Safe test experience on radio active material transport packages," *Radiation Protection*, vol. 38, no. 5, pp. 422–427, 2018.

[3] B. Ma, W. Lou, and X. Yu, "Fragile transportation detecting based on microsystems design with multi-microaccelerometer," *Journal of Transduction Technology*, vol. 15, no. 3, pp. 18–25, 2008.

[4] L. Xu, L. Fang, Z. Ql, X. Li et al., "Design of vibration acceleration measurement system based on MEMS acceleration sensor, instrument technique and sensor," *Instrument Technique and Sensor*, vol. 25, no. 2, pp. 18–21, 2019.

[5] S. Sun, L. Zeng, G. Ll et al., "Regular evaluation and experience feedbacks for PWR fuel assembly transport containers in China," *Packaging Engineering*, vol. 39, no. 23, pp. 105–110, 2018.

[6] L. Xu, L. Fang, and X. Li, "Design of data acquisition system based on MEMS acceleration sensor," *Instrument Technique and Sensor.*, vol. 13, no. 9, pp. 73–95, 2019.

[7] M. Qin, M. Fang, and W. Chen, "Study on measure method of acceleration of wheel in ABSnnn," *Instrument Technique and Sensor*, vol. 15, no. 3, pp. 112–114, 2009.

[8] S. Tan, L. Kai, and D. Bo, "Study on temperature compensation algorithm of piezoelectric pressure sensor," *Piezoelectrics and Acoustooptics*, vol. 41, no. 3, pp. 445–447, 2019.

[9] Z. Nan, Z. Wang, and D. L. Wang, "Attitude algorithm of motion rigid body based on differential equations and acceleration," *Machinery Design & Manufacture*, vol. 5, no. 10, pp. 215–244, 2021.